2024 IEEE International Conference on Robotics and Automation (ICRA 2024)
May 13-17, 2024. Yokohama, Japan

A Force-Controlled Gripper Capable of Measuring Mechanical Properties of an Object

Yi-Shian Tsai, Pin-Chun Yeh, Chun-Hung Huang, I-Cheng Hsueh, and Chao-Chieh Lan, *Senior Member*, *IEEE*

***Abstract*—Various sensorized grippers have been developed to handle delicate objects safely. These grippers have sensors mounted on their fingers' surface that provide direct force measurements. However, multiple sensors are often required on one finger, leading to significant sensor placement and wire routing complexity. Finger-based sensors are limited to sensing external gripping force, and fingers cannot be easily replaced to meet the requirements of objects with specific geometries. To overcome the complexity and limitations of finger surface sensors, this paper proposes a force-controlled two-fingered gripper that relies on the deformation sensing of elastic elements in the drivetrain to obtain finger force. By using a minimum number of optical encoders placed in the drivetrain, accurate position and force sensing can be achieved at any location of each finger. When gripping an object, the size and stiffness of the object can thus be accurately measured. Simulation and experimental results demonstrate the proposed gripper's merits. We expect this new gripper to provide a more competitive solution for robots that need to manipulate objects and check their mechanical qualities at the same time.**

***Index Terms*—Force-controlled gripper, object size and stiffness, planar spring, optical encoder, repeatability.**

I. Introduction

A gripper has been widely used for object manipulation to minimize human labor costs. Industrial applications, such as bin picking, primarily necessitate two-fingered grippers due to their structural simplicity. Replaceable fingers can be used to grip objects of various sizes or objects in hard-to-reach locations. Pneumatic grippers (e.g., [1]) or electric grippers with drivetrains of high gear ratios are employed to reduce the payload to a robot arm without compromising the gripping force. Unlike pneumatic grippers which can only be controlled at a fully open or closed finger position, the finger position of electric grippers can be continuously controlled to meet different object requirements.

Existing research on grippers has focused on designing the fingers' structure to enable stable handling of objects of various sizes and characteristics. Grippers with compliant fingers [2-5] have been developed to adapt to objects with irregular sizes and shapes. While compliant fingers are inherently safe and back-drivable, they have relatively low stiffness in all directions, making it challenging to control finger motion accurately. Placing sensors on highly deformable fingers to achieve gripping force sensing and control is also unreliable. Consequently, self-sensing actuators [6] and vision-based deformation sensing techniques [7] have been developed for grippers with compliant fingers to achieve indirect gripping force sensing and control. To meet the demand for low cost and mechanical reliability, passive grippers with force regulation mechanisms [8] have been developed that do not require sensors. These passive grippers can provide a constant gripping force within a specific range of object size variation.

Direct gripping force measurement and control are necessary for the safe handling of delicate objects. Various types of sensors have been placed on the fingers to ensure direct gripping force measurement. Among them, tactile sensors [9-10], pressure sensors [11], and strain gauges [12] have been used. These types of sensors can provide accurate gripping force sensing. However, the sensor placement and wire routing can cause significant complexity, making grippers unsuitable for use in stringent environments. In particular, tactile sensors are popular but limited to force sensing on the inner side of the finger where they are placed. Additionally, only fingers with flat surfaces can be used to mount tactile sensors. The fingers are not easily replaceable to meet the gripping requirements of non-flat objects.

In addition to controlling the gripping force, sensorized grippers that can identify and recognize the shape of an object have also been investigated [13-15]. Object shape identification allows the gripper to select a stable grasp mode to handle the object with the least uncertainty. However, grippers that can measure mechanical properties of an object are rarely explored. Mechanical properties of an object include its size, stiffness, and compression strength. Unlike the identification of an object shape that does not require very accurate sensors, measurements of an object's mechanical properties require the gripper to have accurate force and position sensing capabilities at the fingers. The size and stiffness measurements of an object can be used for quality checking when the gripper is transferring the object. Thus, additional measuring devices are not required, which leads to a reduction in time and cost in the automation industry. In addition, the measurement of the compression strength of an object can be used to determine the proper gripping force for an unknown fragile object.

This paper aims to develop a force-controlled gripper that can be used to grasp an object and simultaneously measure its mechanical properties. Figs. 1(a) and 1(b) depict the gripper for object size and stiffness measurements, respectively. Using optical encoders to estimate the deformation of the planar springs placed in the drivetrain, gripping force sensing can be achieved at any location of each finger. To minimize the complexity of force sensing and increase the reliability of gripper operation, we place a minimum number of encoders in the drivetrain rather than on the finger surface. In what follows, the prototype of the suggested force-controlled gripper is presented in Sec. II. Sec. III elaborates on the models for finger position and gripping force, which are

This work was supported by the Ministry of Science and Technology, Taiwan (with Project No. NSTC 112-2218-E-006-011). Authors are with the Department of Mechanical Engineering, National Cheng Kung University, Tainan, Taiwan (Corresponding author email: cclan@mail.ncku.edu.tw).

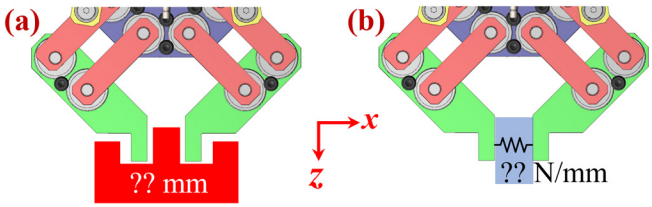

Fig. 1 (a) Object internal and external size measurement (b) Object stiffness measurement

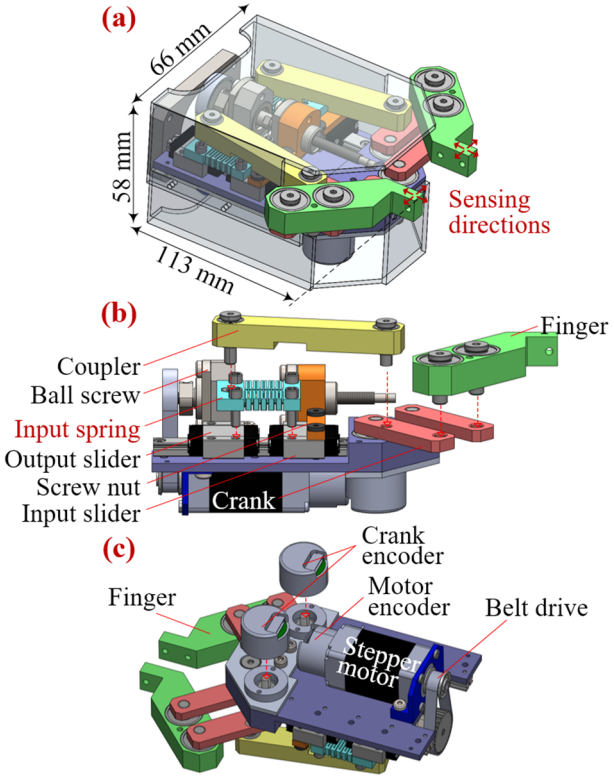

Fig. 2 (a) Prototype of the force-controlled gripper (b) Top view (c) Bottom view

required for determining the gripper dimensions. Additionally, the design and analysis of the planar springs are presented. Using the prototype as an illustration, Sec. IV presents finite element analyses to verify the force-sensing performance of each finger. Experiments are presented in Sec. V to demonstrate that the gripper can be used to accurately obtain the sizes and stiffnesses of various objects. Finally, conclusions are made in Sec. VI.

II. Design Concept and Prototype of the Force-Controlled Gripper

Fig. 2(a) shows a prototype of the proposed force-controlled gripper with dimensions of 113×58×66 mm^3. Figs. 2(b) and 2(c) depict partially exploded top and bottom views, respectively. The gripper is actuated by a stepper motor (PKP214, Oriental Motors) capable of producing a maximum continuous output torque of 0.04 Nm. The motor, located on the bottom side of the gripper, is connected to a ball screw on the top side via a belt drive with a speed ratio of N_b. The ball screw has a pitch of p and a diameter of 4 mm. The ball screw nut is connected to two input sliders on either side of the screw. Each input slider is linked to an output

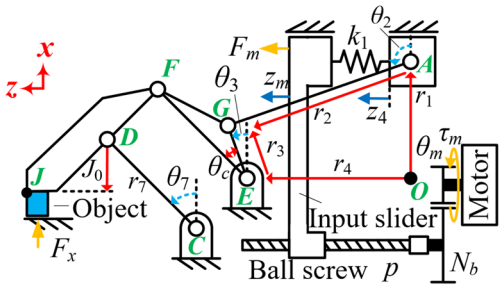

Fig. 3 Symmetric right half of the force-controlled gripper

slider through a planar spring. The movements of the input and output sliders are constrained by the same linear guide. The output slider is further connected to a crank via a coupler, and the crank's rotation serves as input for a parallel four-bar mechanism that provides translational motion for the finger. Finally, the two parallel fingers generate the gripping motion. To minimize friction and clearance during gripping, a journal bearing is used for each revolute joint.

In Fig. 2(c), three identical 15-bit incremental optical encoders are on the bottom side of the gripper. Each encoder has a size of ϕ20×13 mm^3. One of the encoders is the motor encoder, while the other two are the crank encoders used to measure the rotations of the two cranks. These encoders have a resolution of 0.01°, enabling precise sensing and control of finger position. Furthermore, as the encoders are situated in the drivetrain and no sensors are placed on the finger surface, custom-made fingers can be easily mounted on the parallel four-bar mechanisms to handle application-specific objects.

The planar springs on each side of the drivetrain function as force-sensing elements, with their deformation providing information on the finger contact forces in the $\pm\boldsymbol{x}$ and $\pm\boldsymbol{z}$ directions. The motor encoder and crank encoder on each side are used to obtain the deformation of each spring. Despite the use of rigid fingers, the inclusion of springs in the drivetrain makes the gripper inherently compliant with an equivalent stiffness perceived at the fingers. Consequently, the proposed compliant gripper can mitigate unexpected impact forces, in contrast to grippers that solely comprise rigid components.

Encoders have been used in rotary joints to estimate the joint torque (e.g., [16-18]). This paper uses optical encoders to measure and control the position and force of gripper fingers. The proposed gripper allows the use of multiple optical encoders in the drivetrain. In contrast to analog sensors that rely on voltage or current measurements [19-20], optical encoders are more immune to electrical noise interference. Additionally, they are smaller and more cost-effective than grippers that depend on six-axis force/torque sensors.

III. Force and Position Modeling of the Gripper

3.1 Finger gripping force modeling

Fig. 3 shows a schematic of the symmetric right half of the gripper. The motor torque τ_m is evenly distributed to the input force F_m on each input slider as follows.

$$F_m = \pi N_b \tau_m / p \tag{1}$$

where N_b is the speed ratio of the belt drive and p is the pitch of the ball screw. The displacements of the input and output sliders are denoted as z_m and z_4, respectively. The input spring

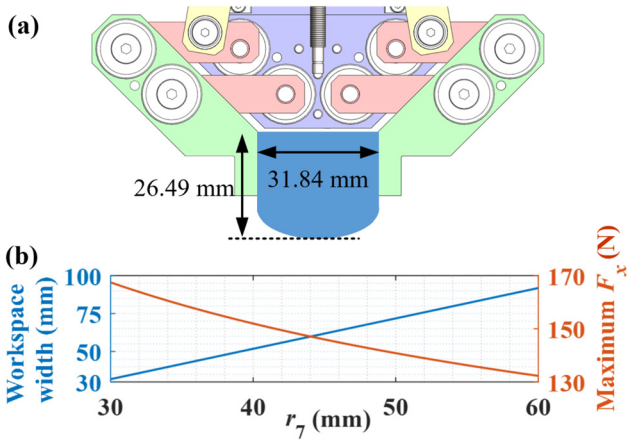

Fig. 4 (a) Gripper workspace (b) Effect of r_7 on the workspace width and maximum gripping force

placed between the two sliders has a stiffness k_1. The input force F_m can be related to the input spring deformation as

$$F_m = k_1(z_m - z_4) \tag{2}$$

Multiplying the motor rotation θ_m by $p/2\pi N_b$, the input slider displacement z_m can be obtained. The output slider displacement z_4 can be related to the rotation θ_3 of line segment ***EG*** as follows.

$$z_4 = r_{40} - r_2 \sin\theta_2 + r_3 \sin\theta_3 \tag{3}$$

where θ_2 is the rotation of the coupler that can be expressed as

$$\theta_2 = \cos^{-1}\left[(r_3 \cos\theta_3 - r_1)/r_2\right] \tag{4}$$

In Eq. (3), r_{40} is the distance between points ***E*** and ***A*** in the ***z*** direction when the rotation θ_7 of the crank is 0°. When $\theta_7 = 0°$, we also have $z_m = z_4 = 0$. The rotation θ_3 is further related to θ_7 by the following.

$$\theta_3 = \theta_7 - \theta_c \tag{5}$$

where θ_c is the angle between line segments ***EG*** and ***EF***.

The fingertip is subjected to external forces F_x in the ***x*** direction. When holding an object as shown in Fig. 3, F_x is used to denote the gripping force from the object to each finger. Through a standard static analysis of the links, the force F_x can be expressed as follows.

$$F_x = -F_m r_3 \sin(\theta_2 - \theta_3) / (r_7 \sin\theta_7 \sin\theta_2) \tag{6}$$

Given the values of z_m and θ_7 from the encoders, the force F_x can be solved. It can be observed in Eq. (6) that F_x only depends on the deformation of the planar spring. Hence, the gripping force is irrelevant to the object's size and stiffness. Due to the symmetry of the gripper, the crank rotation θ_7 should be the same for both fingers.

In Fig. 3, the position of point ***J*** can be expressed as

$$x_J = r_7 \cos\theta_7 - J_0 \tag{7}$$

where J_0 is the relative distance from point ***D*** to ***J*** in the ***x*** direction. The object's size is twice the position of point ***J***.

$$s_o = 2x_J \tag{8}$$

The deformation of the object can be further expressed as

$$x_o = -2r_7(\cos\theta_7 - \cos\theta_{7i}) \tag{9}$$

In Eq. (9), θ_{7i} is the angle of the crank when the finger first contacts the object. The value of θ_{7i} can be obtained at the instant when the values of z_m and z_4 no longer match. Given the gripping force in Eq. (6) and object deformation in Eq. (9), the stiffness of the object can be expressed as

Table 1 Parameters of the proposed gripper

$N_b = 2$, $p = 1$ mm, $r_1 = -0.48$ mm, $r_2 = 52.3$ mm, $r_3 = 10.16$ mm, $r_{40} = 55.87$ mm, $r_7 = 30$ mm, $\theta_c = 25.05°$, $k_1 = 79.25$ N/mm, $J_0 = 22.58$ mm

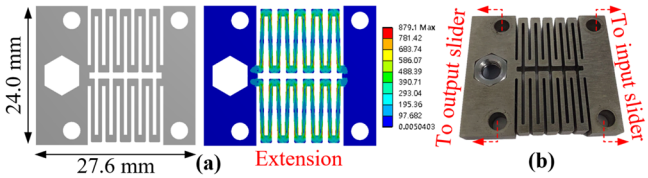

Fig. 5 (a) Original and deformed shapes of the planar spring (b) Prototype of the planar spring

Table 2 Specifications of the planar spring

Specification	Value
Size (mm^3)	24×27.6×4
Mass (g)	14.4
Stiffness (N/mm)	79.25
Max. deformation (mm)	±2
Max. equivalent stress (MPa)	1081.2

$$k_o = dF_x / dx_o \tag{10}$$

The object stiffness may not be constant and depends on the magnitude of object deformation.

3.2 Workspace analysis

Table 1 lists the parameters required in Eqs. (1)-(10). To make the gripper compact, the r_1, r_2, r_3, r_7, and θ_c values were chosen to be small enough without causing drivetrain interference. Considering a drivetrain efficiency of 0.6, the maximum motor torque of 0.04 Nm can be used to deliver an input force of 150 N to each input slider. Fig. 4(a) shows the workspace of the gripper, which has a width of 32 mm and a depth of 27 mm. The workspace corresponds to the range of θ_7 from 0° to 62°. Fig. 4(b) shows the effect of r_7 on the workspace width and maximum gripping force. When the value of r_7 is doubled, the workspace width increases to 92 mm and the maximum gripping force slightly decreases from 168 to 132 N.

3.3 Planar spring design and analysis

As Sec. 3.1 indicates, the deformation measurements of the planar springs are used to obtain the finger gripping force. Elastic elements have been installed in compliant grippers [21-22] and use their deformation to conform to the object shape or estimate the gripper force. The elastic elements used in previous work were mainly coil springs. The size of the coil springs cannot be easily minimized. In this paper, we propose the use of planar springs as the elastic elements. The specifications of the planar spring are listed in Table 2. Fig. 5(a) shows the original and 2-mm extended shapes of the planar spring, whereas Fig. 5(b) shows the prototype of the planar spring. The holes at the four corners of the spring are used to connect the input and output sliders. The spring has a thin and planar structure that can be easily accommodated in the drivetrain. The shape of the spring is winded such that the spring achieves a reaction force of nearly 150 N when the maximum extension of 2 mm is applied. Meanwhile, the maximum equivalent stress is minimized. The Generalized

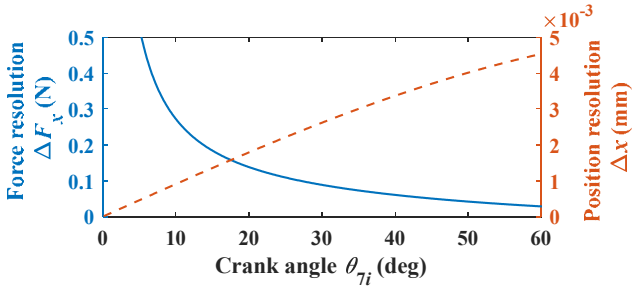

Fig. 6 Resolution of finger force and position measurement

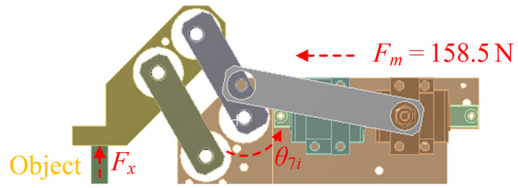

Fig. 7 Finite element model of the gripping force simulation

Multiple Shooting Method [23] was used to facilitate the design of the spring shape.

Heat-treated plastic mold steel (S-STAR-A) is used as the material for the planar springs. The planar spring is fabricated using wire electrical discharge machining. When the maximum deformation of the planar spring is reached, the maximum equivalent stress is 1081.2 MPa for the planar spring. The maximum equivalent stress is smaller than the yield stress of the material (1540 MPa).

IV. Verification of the Finger Position and Force

4.1 Finger position and force resolution analysis

The finger position and force sensing resolutions in the ***x*** direction depend on the resolutions of the motor and crank encoders. For the 15-bit motor encoder, a motor rotation step of 0.01° converts to a crank rotation of 0.000245°, which is very small. Hence, the finger position and force sensing resolutions mainly depend on the resolution of the crank encoder. Using a step of 0.01° for the crank rotation, the finger position resolution can be obtained using Eq. (7). The right vertical axis of Fig. 6 shows the finger position resolution in the ***x*** direction. The resolution depends on the crank angle and the maximum resolution value is 4.5 μm when the crank angle is at 60°. Hence, the fingers have very high position resolution, which is required to achieve accurate measurement of an object's mechanical properties.

The finger force resolution can also be obtained similarly. A rotation step of 0.01° is given to the crank such that $\theta_7 = \theta_{7i} + 0.01°$. Based on Eq. (6), the increment of the gripping force is denoted as ΔF_x. The magnitude of ΔF_x can be viewed as the finger force resolution in the ***x*** direction. The left vertical axis of Fig. 6 shows the finger force resolution in the ***x*** direction. The gripping force resolution is less than 0.25 N for a crank angle larger than 10°, which accounts for only 0.15% of the maximum gripping force. When the crank angle is less than 10°, the force resolution drastically increases due to the force singularity at $\theta_7 = 0°$. Hence, the gripper should be operated away from $\theta_7 = 0°$.

4.2 Finite element verification of gripping force sensing

The solid model in Fig. 2(a) was imported into ANSYS to verify the sensing of finger gripping force with a rigid object.

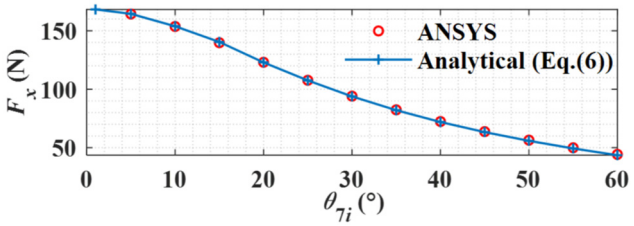

Fig. 8 Comparison of analytical and simulation results of gripping force F_x

Fig. 7 illustrates the finite element model in ANSYS where the crank angle is at $\theta_{7i} = 30°$. To accurately account for the deformation of the planar spring, a large deflection analysis was used. All other links in the gripper were treated as rigid. All the revolute and sliding joints were assumed frictionless. The input slider on each side of the gripper was given a force of F_m = 158.5 N, which was used to emulate the maximum force the motor can provide. This maximum force corresponds to the input spring deformation of 2 mm. The reaction force from the rigid object was obtained. Fig. 8 shows the curves of gripping force with respect to different crank angles. The analytical curve is obtained using Eq. (6). The maximum difference between the ANSYS results and the analytical curve is less than 1%. According to the comparison of Eq. (6) and ANSYS simulation, the gripping force is valid regardless of the location of the object in the ***z*** direction.

The analytical curve shown in Fig. 8 also represents the maximum gripping force with respect to the initial crank angle. It can be observed that the maximum gripping force increases with the decrease of θ_{7i}. The maximum gripping force is 168 N when θ_{7i} is nearly 0°. When $\theta_{7i} = 60°$, the maximum gripping force can still achieve 44 N.

4.3 Gripping force controller

Based on Eq. (6), the gripping force is indirectly controlled by controlling the input force F_m. Using Eq. (2), a position controller is developed to control the relative displacement between z_m and z_4 to control F_m. The controller gains were tuned to ensure gripping stability. Similar controllers can be found in our previous work on series elastic actuators [24-25].

V. Experimental Validations

5.1 Finger position and force repeatability tests

Fig. 9(a) shows a prototype of the gripper. The total mass of the gripper is 0.75 kg. The size of the gripper is 113×58×66 mm^3. Finger position repeatability is important for grippers that need to measure the size and stiffness of an object. Fig. 9(b) shows the experimental setup of the finger position repeatability. Two laser displacement sensors (FASTUS CD22-15) with a sensitivity of 1 μm were used to measure the position variations of one finger in the ***x*** and ***z*** directions. The other finger was temporarily removed to avoid measurement interference. The gripper was controlled to move periodically between $\theta_7 = 15°$ to $\theta_7 = 50°$. The distance between the two points is 9.70 mm. The finger position variations in the ***x*** and ***z*** directions at $\theta_7 = 50°$ were recorded. A total of 30 cycles were tested. Fig. 10 shows the values of the finger ***x*** and ***z*** positions. In each direction, the average of the position values is subtracted from the position values to clearly compare the variation. According to the formulas defined in the ISO 9283

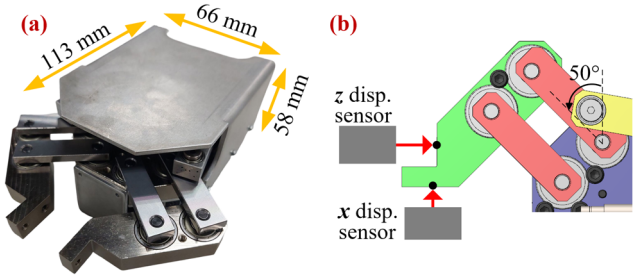

Fig. 9 (a) Prototype of the gripper (b) Experimental setup of finger position repeatability

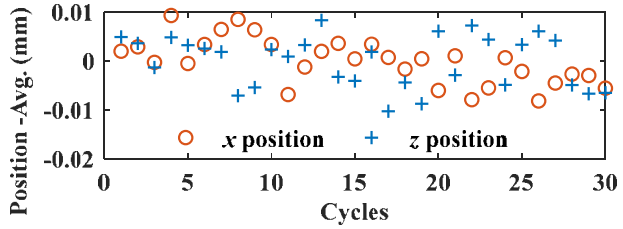

Fig. 10 Experimental results of finger position repeatability

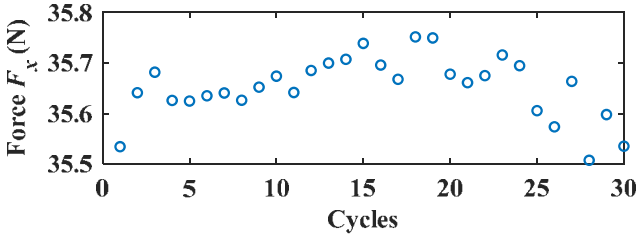

Fig. 11 Experimental results of finger gripping force repeatability ($\theta_{7i} = 45°$)

standard [26], the repeatability of the finger position is 0.012 mm in the ***x*** direction and 0.012 mm in the ***z*** direction. Hence, the use of compliance in the drivetrain of our gripper does not affect the positioning repeatability of the finger.

A similar experiment was conducted to measure the force control repeatability of the proposed gripper. A loadcell (Futek LLB250) was placed in the middle of the two fingers to measure the gripping force F_x. The readings from the loadcell were used as the ground truth to verify the force calculated using Eq. (6). A closed-loop controller was developed for the motor to give the input slider a displacement of Δz_m = 1 mm with a constant speed of 1.5 mm/s. After 1.5 s, the input slider returned to Δz_m = 0 mm to complete one cycle. Fig. 11 shows the experimental results of 30 cycles based on the loadcell values. The average value of F_x is 35.65 N from the loadcell sensing. According to ISO 9283 [26], the repeatability of the gripping force control is 0.16 N.

5.2 Object size measuring test

Fig. 12(a) illustrates the gripper grasping a bearing and simultaneously measuring its outer diameter. An experiment has been conducted to verify the accuracy and precision of the gripper's ability to measure the size of an object. Bearings of three different sizes were used for the experiment. Fig. 12(b) shows the sizes of the bearings. Table 3 lists the outer diameter of each bearing for gripping. Three measurements were made for each bearing. To ensure the accuracy of size measurement, the gripping force was controlled at 4 N for

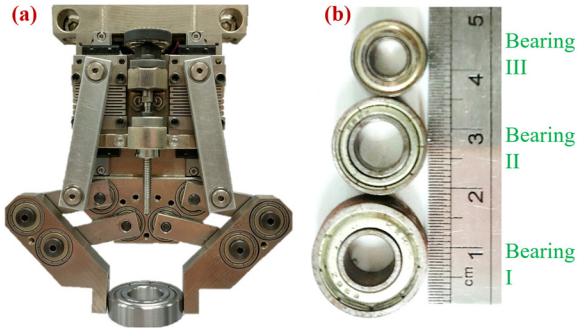

Fig. 12 (a) Gripper grasping and measuring the size of a bearing (b) Bearings of different sizes

Table 3 Results of bearing diameter measurements (mm)

	Bearing I	Bearing II	Bearing III
Nominal outer diameter	19.00	16.00	13.00
1st measurement	19.02	15.96	13.03
2nd measurement	19.02	15.96	13.03
3rd measurement	19.02	15.96	13.03

each bearing. The size of the bearing is obtained using Eq. (8). For all bearings, the maximum measurement error is 0.04 mm, which is smaller than the reading error of metric Vernier calipers. The three measurements for each bearing are the same, indicating the precision of object size measurements using the proposed gripper is less than 0.01 mm. Additional tests can be made to measure the inner diameter of each bearing. To measure the inner diameter accurately, the finger jaws should be replaced by those that can geometrically fit the inner ring of a bearing.

5.3 Object stiffness measuring test

Fig. 13(a) illustrates the gripper grasping an object and simultaneously measuring its stiffness. An experiment has been conducted to demonstrate the gripper's ability to measure the stiffness of an object. As shown in Fig. 13(a) and listed in Table 4, objects of four different hardness values were used in the experiment. The sizes of the objects are all 30×20×10 mm^3. Fig. 14 shows the measured stiffness curves when a force of 20 N is given to deform each object. Objects I and II have high stiffness values and their stiffness curves are linear. Objects III and IV have low stiffness values and their stiffness curves begin with a nonlinear segment and gradually become linear in the large-deformation range. A linear fitting line is obtained for each stiffness curve in Fig. 14. The slope of each fitting line represents the stiffness of the associated object and is listed in Table 4. The proposed gripper has a wide stiffness measuring range from 5 to 332 N/mm. By measuring the stiffness, it is possible to identify the material of the object.

5.4 Demonstration of testing and gripping fragile objects

The proposed gripper can sense and control the gripping force on objects of different shapes and stiffnesses. A cookie as shown in Fig. 15(a) is used as a fragile object for gripping demonstration. The fracturing force of the cookie is not known in advance. Hence, it is difficult to determine the force that can stably grip the cookie without fracture. Fig. 15(b) shows the curve of gripping force to object deformation for the cookie in Fig. 15(a). This curve was obtained by using the

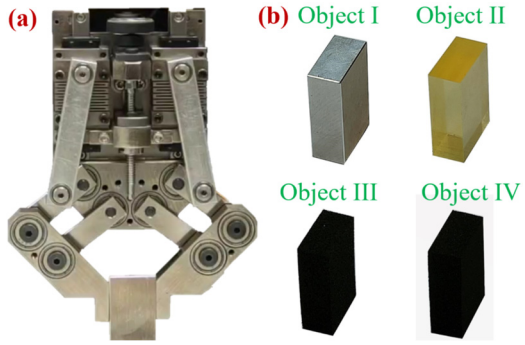

Fig. 13 (a) Gripper grasping and measuring the stiffness of an object (b) Objects of different stiffnesses

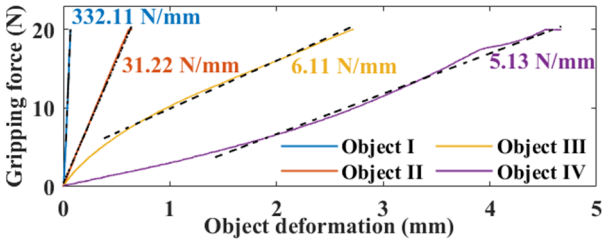

Fig. 14 Experimental stiffness curves of four objects

Table 4 Results of object stiffness measurements

	Material	Measured stiffness
Object I	Aluminum alloy 6061	332.11 N/mm
Object II	Urethane (A30)	31.22 N/mm
Object III	Sponge (ASKER C30)	6.11 N/mm
Object IV	Sponge (ASKER C8)	5.13 N/mm

proposed gripper to squeeze the cookie and sense its deformation and gripping force. In Zone I of Fig. 15(b), the curve is linear with a slope of 15.77 N/mm. The slope represents the stiffness of the cookie in its elastic region. In Zone II, the curve flattens, indicating that the cookie starts to fracture. The fracturing force can be defined as the maximum gripping force in Zone II, which is 11.47 N. Fig. 15(c) shows the fractured cookie. In Zone III, the cookie starts to collapse so that the gripping force reduces to zero. The proposed gripper can be used to accurately obtain the stiffness and fracturing force of a fragile object, which helps in determining the suitable gripping force. A gripping force in Zone I can be used to avoid fracturing the cookie. As an example, Fig. 15(d) shows the result of controlling the gripping force at 2.67 N. The cookie can be stably gripped. The measured stiffness can also be used to assess the quality variation among different objects.

5.5 Merits of the proposed force-controlled gripper

Based on the parameters in Table 1, Table 5 lists the specifications of the proposed gripper. Except for the specifications of mass and dimension, all other specifications refer to the performance of one finger. The position and force resolutions are verified in Sec. 4.1. The maximum force is verified in Sec. 4.2. The position and force repeatability values are verified in Sec. 5.1.

Comparisons with commercial grippers capable of finger force sensing are made in Table 5. The two-fingered gripper in [27] is based on a six-axis force sensor placed on the inner side of each fingertip so that both forces in the x and z

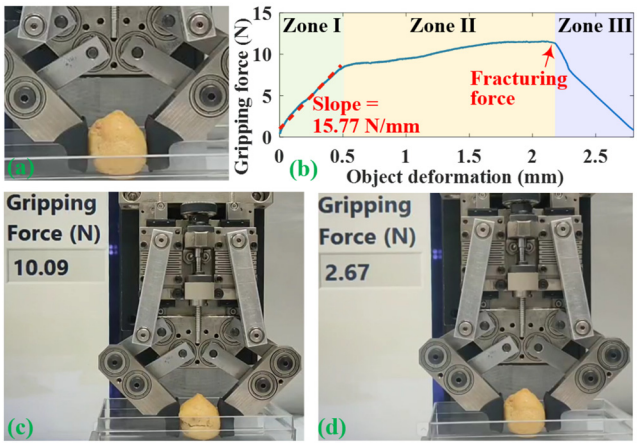

Fig. 15 (a) Gripping a fragile cookie (b) Gripping force to deformation curve (c) Fractured cookie (d) Stable gripping

Table 5 Specifications of the proposed gripper and comparison with existing grippers

	Our gripper	RG2-FT [27]	2F-85 [28]
Total mass (kg)	0.75	0.98	0.93
Dimension (mm^3)	113×58×66	219×149×49	153×ϕ75
Crank length (mm)	30	55	57.4
Crank rotation (°)	62	50	45
Position resolution (mm)	0.005	0.1	0.4
Position repeatability (mm)	0.01	0.1	0.05
Maximum x force (N)	168	40	235
x force resolution (N)	0.25	0.4	N/A
x force repeatability (N)	0.16	N/A	±10%
External/internal gripping	Yes/Yes	Yes/No	Yes/Yes

directions can be sensed. The gripper in [28] is based on motor current sensing. Hence, only the gripping force can be sensed and controlled. Although the proposed gripper is compliant and the grippers in [27-28] are rigid, the proposed gripper can provide much better finger position resolution and repeatability than those in [27-28] due to the use of high-resolution encoders and a drivetrain of low backlash. The force sensing range, resolution, and repeatability of our proposed gripper are also superior to those in [27-28] due to the use of planar springs in the drivetrain.

VI. Conclusions

This paper has presented a force-controlled two-fingered gripper capable of measuring mechanical properties of an object. By using three optical encoders to measure the deformations of the planar springs in the drivetrain and rotations of the cranks, the gripping force and object deformation can be independently estimated. The planar springs are specifically designed to be compact. Compared with commercially available sensorized grippers, the design of the proposed gripper significantly reduces the complexity of finger force sensing. Additionally, fingers can be easily replaced to meet specific gripping requirements. The experimental results show that the size and stiffness of an object can be accurately measured while grasping the object. It is expected that this gripper can be applied to facilitate the manipulation and quality check of different objects.

REFERENCES

[1] C.-C. Chen and C.-C. Lan, 2017, "An accurate force regulation mechanism for high-speed handling of fragile objects using pneumatic grippers," IEEE Transactions on Automation Science and Engineering, 15(4), 1600-1608.

[2] C.-C. Lan and K.-M. Lee, 2008, "An analytical contact model for design of compliant fingers," ASME Journal of Mechanical Design, 130(1), 011008.

[3] S. D'Avella, M. Fontana, R. Vertechy, and P. Tripicchio, 2022 "Towards autonomous soft grasping of deformable objects using flexible thin-film electro-adhesive gripper," IEEE International Conference on Automation Science and Engineering, 1309-1314.

[4] A. Milojević, S. Linß, and H. Handroos, 2021, "Soft robotic compliant two-finger gripper mechanism for adaptive and gentle food handling," IEEE International Conference on Soft Robotics, 163-168.

[5] Y. Sun, Y. Liu, F. Pancheri, and T. C. Lueth, 2022, "Larg: A lightweight robotic gripper with 3-d topology optimized adaptive fingers," IEEE/ASME Transactions on Mechatronics, 27(4), 2026-2034.

[6] C.-C. Lan and C.-H. Fan, 2010, "Investigation on pretensioned shape memory alloy actuators for force and displacement self-sensing," IEEE/RSJ International Conference on Intelligent Robots and Systems, 3043-3048.

[7] W. Xu, H. Zhang, H. Yuan, and B. Liang, 2021, "A compliant adaptive gripper and its intrinsic force sensing method," IEEE Transactions on Robotics, 37(5), 1584-1603.

[8] J.-Y. Wang and C.-C. Lan, 2014, "A constant-force compliant gripper for handling objects of various sizes," ASME Journal of Mechanical Design, 136(7), 071008.

[9] Y. She, S. Wang, S. Dong, N. Sunil, A. Rodriguez, and E. Adelson, 2021, "Cable manipulation with a tactile-reactive gripper," The International Journal of Robotics Research, 40(12-14), 1385-1401.

[10] K. Sasaki, K. Koyama, A. Ming, M. Shimojo, R. Plateaux, and J.-Y. Choley, 2018, "Robotic grasping using proximity sensors for detecting both target object and support surface," IEEE/RSJ International Conference on Intelligent Robots and Systems, 2925-2932.

[11] C. Tawk, H. Zhou, E. Sariyildiz, M. In Het Panhuis, G. M. Spinks, and G. Alici, 2020, "Design, modeling, and control of a 3D printed monolithic soft robotic finger with embedded pneumatic sensing chambers," IEEE/ASME Transactions on Mechatronics, 26(2), 876-887.

[12] S. Hogreve and K. Tracht, 2014, "Design and implementation of multiaxial force sensing gripper fingers," Production Engineering, 8, 765-772.

[13] C.-W. Hung, S.-X. Zeng, C.-H. Lee, and W.-T. Li, 2021, "End-to-end deep learning by MCU implementation: an intelligent gripper for shape identification," Sensors 21(3), 891.

[14] W.-H. Qian, H. Qiao, and S. K. Tso, 2001, "Synthesizing two-fingered grippers for positioning and identifying objects," IEEE Transactions on Systems, Man, and Cybernetics, Part B (Cybernetics), 31(4), 602-615.

[15] R. Zuo, Z. Zhou, B. Ying, and X. Liu, 2021, "A soft robotic gripper with anti-freezing ionic hydrogel-based sensors for learning-based object recognition," IEEE International Conference on Robotics and Automation, 12164-12169.

[16] Y.-L. Yu and C.-C. Lan, 2019, "Design of a miniature series elastic actuator for bilateral teleoperations requiring accurate torque sensing and control," IEEE Robotics and Automation Letters, 4(2), pp.500-507.

[17] C.-C. Chung, C.-H. Huang, and C.-C. Lan, 2022, "A torque-controlled actuator with high rigidity and low aspect ratio," IEEE/ASME Transactions on Mechatronics, 27(6), 5572-5582.

[18] C.-H. Huang, K.-W. Chiao, C.-P. Yu, Y.-C. Kuo, and C.-C. Lan, 2023," A variable-stiffness robot for force-sensitive applications," IEEE/ASME Transactions on Mechatronics, 28(4), 1862-1870.

[19] M. Guo, P. Wu, B. Yi, D. Gealy, S. McKinley, and P. Abbeel, 2019, "Blue gripper: a robust, low-cost, and force-controlled robot hand," IEEE International Conference on Automation Science and Engineering, 1505-1510.

[20] F. Ostyn, B. Vanderborght, and G. Crevecoeur, 2022, "Design and control of a quasi-direct drive robotic gripper for collision tolerant picking at high speed," IEEE Robotics and Automation Letters, 7(3), 7692-7699.

[21] O. Kaya, G. B. Tağlıoğlu, and Ş. Ertuğrul, 2022, "The series elastic gripper design, object detection, and recognition by touch," Journal of Mechanisms and Robotics, 14(1), 014501.

[22] Y. Yan, S. Guo, C. Lyu, D. Zhao, and Z. Lin, 2022, "SEA-based humanoid finger-functional parallel gripper with two actuators: PG2 gripper," IEEE Transactions on Instrumentation and Measurement, 72, 3000213.

[23] C.-C. Lan, K.-M. Lee, and J.-H. Liou, 2009, "Dynamics of highly elastic mechanisms using the generalized multiple shooting method: simulations and experiments," Mechanism and Machine Theory, 44(12), 2164-2178.

[24] K.-Y. Lin, C.-C. Chung, and C.-C. Lan, 2020, "Improving the dynamic force control of series elastic actuation using motors of high torque-to-inertia ratios," IEEE Access, 8, 6968-6977.

[25] K.-Y. Wu, Y.-Y. Su, Y.-L. Yu, K.-Y. Lin, and C.-C. Lan, 2017, "Series elastic actuation of an elbow rehabilitation exoskeleton with axis misalignment adaptation," International Conference on Rehabilitation Robotics, 567-572.

[26] ISO 9283, 1998, "Manipulating industrial robots–performance criteria and related test methods," International Organization of Standards, 7-2.

[27] https://onrobot.com/en/products/rg2-ft-gripper

[28] https://robotiq.com/products/2f85-140-adaptive-robot-gripper